

Absence of Phase Transition for Antiferromagnetic Potts Models via the Dobrushin Uniqueness Theorem

Jesús Salas
Alan D. Sokal
Department of Physics
New York University
4 Washington Place
New York, NY 10003 USA
SALAS@MAFALDA.PHYSICS.NYU.EDU, SOKAL@NYU.EDU

June 11, 2018

Dedicated to the memory of R.L. Dobrushin

Abstract

We prove that the q -state Potts antiferromagnet on a lattice of maximum coordination number r exhibits exponential decay of correlations uniformly at all temperatures (including zero temperature) whenever $q > 2r$. We also prove slightly better bounds for several two-dimensional lattices: square lattice ($q \geq 7$), triangular lattice ($q \geq 11$), hexagonal lattice ($q \geq 4$), and Kagomé lattice ($q \geq 6$). The proofs are based on the Dobrushin uniqueness theorem.

Key Words: Dobrushin uniqueness theorem, antiferromagnetic Potts models, phase transition.

1 Introduction

Dobrushin’s uniqueness theorem [1, 2, 3, 4] provides a simple but powerful method for proving the uniqueness of the infinite-volume Gibbs measure, as well as the exponential decay of correlations in this unique Gibbs measure, for classical-statistical-mechanical systems deep in a single-phase region. The basic idea underlying this theorem is that if the probability distribution of a single spin σ_i depends “sufficiently weakly” on the remaining spins $\{\sigma_j\}_{j \neq i}$, then one can deduce (by a clever iterative argument) uniqueness of the Gibbs measure and exponential decay of correlations.

The principal applications of this method have been in two regimes:

- 1) *High temperature.* Here σ_i depends weakly on the $\{\sigma_j\}_{j \neq i}$ because of the strong thermal fluctuations.
- 2) *Large magnetic field.* Here σ_i tends to follow the magnetic field, no matter what the other spins are doing; so the probability distribution of σ_i again depends weakly on the $\{\sigma_j\}_{j \neq i}$.

However, Kotecký (cited in [3, pp. 148–149, 457]) has pointed out that Dobrushin’s theorem is applicable also in a third regime:

- 3) *High entropy.* Here σ_i has so many states available to it (with equal or almost equal probability), no matter what the other spins are doing, that its probability distribution again depends weakly on the $\{\sigma_j\}_{j \neq i}$.

The simplest example of this situation is the antiferromagnetic q -state Potts model [5, 6, 7]

$$\mathcal{H} = -J \sum_{x \sim y} \delta_{\sigma_x \sigma_y} \tag{1.1}$$

with $J = -\beta < 0$, on a lattice in which each site has r nearest neighbors.¹ Even at zero temperature ($J = -\infty$), the spin σ_i is required only to be different from all the neighboring spins $\{\sigma_j\}_{j \sim i}$. If $q \gg r$, then the probability distribution of σ_i depends only weakly on the values of the $\{\sigma_j\}_{j \sim i}$. It turns out that Dobrushin’s theorem is applicable whenever $q > 2r$ (see Section 3 below), as well as in some additional cases (see Sections 4 and 5). Thus, for q sufficiently large (how large depends on the lattice under consideration), the q -state Potts antiferromagnet has a unique Gibbs measure and exponential decay of correlations at all temperatures, *including zero temperature*: the system is disordered as a result of entropy.

More precisely, we expect that for each lattice \mathcal{L} there will be a value $q_c(\mathcal{L})$ such that

- (a) For $q > q_c(\mathcal{L})$ the model has exponential decay of correlations uniformly at all temperatures, including zero temperature.

¹We use the notation $x \sim y$ to indicate that x is a nearest neighbor of y . The sum in (1.1) thus runs over all nearest-neighbor pairs of lattice sites (each pair counted once), and each spin takes values $\sigma_x \in \{1, 2, \dots, q\}$. The antiferromagnetic case corresponds to $J = -\beta < 0$.

- (b) For $q = q_c(\mathcal{L})$ the model has a critical point at zero temperature.
- (c) For $q < q_c(\mathcal{L})$ any behavior is possible. Often (though not always) the model has a phase transition at nonzero temperature, which may be of either first or second order.²

Here is what is believed to be true for the standard two-dimensional lattices:

Square lattice. Baxter [10, 11] has determined the exact free energy (among other quantities) for the square-lattice Potts model on two special curves in the (J, q) -plane (see Figure 1):

$$e^J = 1 \pm \sqrt{q} \tag{1.2}$$

$$e^J = -1 \pm \sqrt{4 - q} \tag{1.3}$$

Curve (1.2₊) is known to correspond to the ferromagnetic critical point, and Baxter [11] has conjectured that curve (1.3₊) corresponds to the antiferromagnetic critical point. For $q = 2$ this gives the known exact value [12]; for $q = 3$ it predicts a zero-temperature critical point ($J_c = -\infty$), in accordance with previous belief [13, 14]³; and for $q > 3$ it predicts that the putative critical point lies in the unphysical region ($e^{J_c} < 0$), so that the entire physical region $-\infty \leq J \leq 0$ lies in the disordered phase. These predictions for $q = 3, 4$ have recently been confirmed by high-precision Monte Carlo simulation [19]. For some further interesting speculations, see [20, 21].

Triangular lattice. Baxter and collaborators [22, 23, 24] have determined the exact free energy (among other quantities) for the triangular-lattice Potts model on two special curves in the (J, q) -plane (see Figure 2):

$$(e^J - 1)^2 (e^J + 2) = q \tag{1.4}$$

$$e^J = 0 \quad \text{for } 0 < q < 4 \tag{1.5}$$

The uppermost branch of curve (1.4) is known to correspond to the ferromagnetic critical point [22], and Baxter [23] has conjectured that (1.5) corresponds to the antiferromagnetic critical point. This prediction of a zero-temperature critical point is known to be correct for $q = 2$ [8], and there is heuristic analytical evidence that it is correct also for $q = 4$ [18, 25]. On the other hand, for $q = 3$ this prediction contradicts the rigorous result [26], based on Pirogov-Sinai theory, that there is a low-temperature phase with long-range order and small correlation length. Indeed, a recent Monte Carlo study of the $q = 3$ model has found strong evidence for a first-order transition (to an ordered phase) at $\beta \approx 1.594$ [27]. For $q > 4$ one may expect that the triangular-lattice Potts model is noncritical even at zero temperature.

²Exceptions to the usual behavior are, for example, the Ising model ($q = 2$) on the triangular lattice ($q_c = 4$), which has a zero-temperature critical point [8]; and the Ising model on the Kagomé lattice ($q_c = 3$), which is non-critical at all temperatures, including zero temperature [9].

³Note also that the $q = 3$ model is exactly soluble at zero temperature in an arbitrary magnetic field [14, 15, 16, 17]; this might increase one's suspicions that the zero-temperature zero-field case is critical. Indeed, Henley [18] has some very interesting predictions for the critical exponents.

Finally, the physical meaning of the two lower branches of (1.4) is mysterious. The lowermost branch of (1.4) lies entirely in the unphysical region $e^J < 0$. The middle branch is located in the antiferromagnetic region for $0 < q < 2$, and in the unphysical region for $q > 2$; at $q = 2$ it coincides with the antiferromagnetic critical point. For some further interesting speculations, see [20].

Hexagonal lattice. This lattice is connected by duality [10] with the triangular lattice⁴; the image of (1.4)/(1.5) is

$$(e^J - 1)^3 - 3q(e^J - 1) - q^2 = 0 \quad (1.6)$$

$$e^J = 1 - q \quad \text{for } 0 < q < 4 \quad (1.7)$$

Curve (1.6) has three branches in the region $q \geq 0$ (see Figure 3): the uppermost branch (with $0 \leq q < \infty$ and $e^J \geq 1$) is the ferromagnetic critical point; the middle branch (with $0 \leq q \leq 4$ and $-1 \leq e^J \leq 1$) contains the antiferromagnetic Ising critical point ($q = 2$, $e^J = 2 - \sqrt{3}$) and crosses the zero-temperature point $e^J = 0$ at $q = (3 + \sqrt{5})/2 \approx 2.618$; while the lowermost branch crosses the zero-temperature point $e^J = 0$ at $q = (3 - \sqrt{5})/2 \approx 0.382$.⁵ The meaning of this lowermost branch is mysterious, as is the meaning of (1.7). But the behavior of the middle branch suggests that it may be the antiferromagnetic critical curve: in this case there would be a zero-temperature critical point for $q = (3 + \sqrt{5})/2$ [if this assertion has any meaning⁶], and the model would be disordered even at zero temperature for $q > (3 + \sqrt{5})/2$. For some further interesting speculations, see [20].

Kagomé lattice. This is not merely an academic example, as some condensed-matter systems (for instance, the insulator $\text{SrCr}_{8-x}\text{Ga}_{4-x}\text{O}_{19}$) have the Kagomé lattice structure [32, 33, 34]. For $q = 2$ this model has been solved exactly [9], and there is no phase transition at any temperature. For $q = 3$ the zero-temperature model can be mapped onto the zero-temperature 4-state triangular-lattice Potts antiferromagnet [25] and so is expected to be critical [18, 35]. For $q > 3$ one may expect that this model is noncritical even at zero temperature.

In Table 1 we summarize the believed exact values of $q_c(\mathcal{L})$ for these four lattices, along with the upper bounds that follow from our computer-assisted proofs. Clearly, our rigorous bounds still fall far short of what is believed to be true in most of the

⁴Furthermore, the hexagonal-lattice Potts model *on the curve (1.6)* (and only there) can be mapped via the star-triangle transformation onto a triangular-lattice Potts model, which turns out to lie exactly on the curve (1.4).

⁵The middle branch is missing in [20, p. 673, Figure 8].

⁶The Potts models for noninteger q can be given a rigorous meaning via the mapping onto the Fortuin-Kasteleyn random-cluster model [28, 29, 30]. The trouble is that in the antiferromagnetic case ($J < 0$) this latter model has negative weights, and so cannot be given a standard probabilistic interpretation. In particular, the existence of a good infinite-volume limit is problematical; the limit could depend strongly on the subsequence of lattice sizes and on the boundary conditions. The same is true of the “anti-Fortuin-Kasteleyn” representation, in which the coefficients are products of chromatic polynomials of clusters: again the weights can be negative for non-integer q , and the existence of the infinite-volume limit is problematical. Likewise, the ice-model representation [10, 31] has in general complex weights for $0 < q < 4$, even in the ferromagnetic case.

lattices considered here. Only for the hexagonal lattice are we somewhat close to the expected result.

The plan of this paper is as follows: In Section 2 we set the notation and recall the Dobrushin uniqueness theorem. In Section 3 we prove that the Dobrushin uniqueness theorem is applicable to the q -state Potts antiferromagnet on a lattice of maximum coordination number r , uniformly at all temperatures (including zero temperature), whenever $q > 2r$. In Section 4 we improve this result for some common lattices (square, hexagonal, triangular, and Kagomé), using a single-site decimation scheme and a computer-assisted proof. Finally in Section 5 we improve our results for the hexagonal and Kagomé lattices using more sophisticated decimation schemes.

During the preparation of this paper we learned of the tragic death of Professor Dobrushin, one of the founders of and main contributors to modern mathematical statistical mechanics. We dedicate this paper to his memory.

2 Notation and Preliminaries

2.1 Basic Setup

The basic framework for all our results is the Dobrushin–Lanford–Ruelle (DLR) approach to the equilibrium statistical mechanics of infinite-volume classical lattice systems. A pedagogical introduction to this theory can be found in [36, Sections 2.1–2.3]; detailed expositions can be found in the books of Preston [37], Georgii [3] and Simon [4]. Here we summarize very briefly the notation and the basic ideas. The central idea in the DLR theory is to define an *infinite-volume Gibbs measure* as a probability distribution for the infinite-volume system whose *conditional* probabilities for *finite* subsystems are given by the Boltzmann–Gibbs formula for the given formal Hamiltonian.

Consider a classical-statistical-mechanical system on a countably infinite lattice \mathcal{L} , with spin variables σ_i ($i \in \mathcal{L}$) taking values in some state space E .⁷ The equilibrium statistical mechanics of such a system is defined by a *specification* $\Pi = \{\pi_\Lambda\}_{\Lambda \text{ finite } \subset \mathcal{L}}$: here $\pi_\Lambda(\sigma_\Lambda | \sigma_{\Lambda^c})$ gives the conditional probability distribution for the spin configuration $\sigma_\Lambda \equiv \{\sigma_i\}_{i \in \Lambda}$ *inside* the finite set Λ , given the spin configuration $\sigma_{\Lambda^c} \equiv \{\sigma_i\}_{i \in \Lambda^c}$ *outside* Λ . The $\{\pi_\Lambda\}$ have to satisfy various consistency conditions [3, 36, 37]. We shall further assume that each kernel π_Λ is *quasilocal* [3, 36]: this is a very mild decay condition on the long-range interactions.

Usually the specification $\{\pi_\Lambda\}$ is defined via an *interaction* (= “formal Hamiltonian”) $\Phi = \{\Phi_A\}_{A \text{ finite } \subset \mathcal{L}}$: here Φ_A is, roughly speaking, the elementary contribution to the Hamiltonian coming from the finite set of spins $A \subset \mathcal{L}$. Thus, the Hamiltonian

⁷In all the applications in this paper, the state space E will be the *finite* set $\{1, \dots, q\}$. However, the Dobrushin uniqueness theorem is valid in much greater generality.

H_Λ^Φ for volume Λ with external condition σ_{Λ^c} is

$$H_\Lambda^\Phi(\sigma_\Lambda|\sigma_{\Lambda^c}) = \sum_{\substack{A \text{ finite } \subset \mathcal{L} \\ A \cap \Lambda \neq \emptyset}} \Phi_A(\sigma_\Lambda, \sigma_{\Lambda^c}). \quad (2.1)$$

The kernel π_Λ is then, by definition, the corresponding Boltzmann-Gibbs measure:

$$\pi_\Lambda^\Phi(\sigma_\Lambda|\sigma_{\Lambda^c}) = Z_\Lambda^\Phi(\sigma_{\Lambda^c})^{-1} \exp[-H_\Lambda^\Phi(\sigma_\Lambda|\sigma_{\Lambda^c})] \prod_{i \in \Lambda} d\mu^0(\sigma_i), \quad (2.2)$$

where μ^0 is the *a priori* single-spin distribution. Under mild summability conditions on the interaction $\{\Phi_A\}$, it can be shown that (2.1)/(2.2) are well-defined and satisfy all the conditions for a specification, and furthermore that the π_Λ are quasilocal [3, 36]. (In this paper all interactions will be finite-range, so the requisite conditions will hold trivially.)

Finally, a probability measure μ on the configuration space of the infinite-volume system is said to be an *infinite-volume Gibbs measure* for the specification Π if, for each finite subset $\Lambda \subset \mathcal{L}$, the conditional probability distribution $\mu(\cdot|\sigma_{\Lambda^c})$ equals $\pi_\Lambda(\cdot|\sigma_{\Lambda^c})$. See [3, 36, 37] for details.

2.2 Dobrushin's Uniqueness Theorem

Let us now focus on the kernels $\pi_{\{i\}}$ ($i \in \mathcal{L}$), which give the probability distribution of a *single* spin σ_i conditional on the remaining spins $\{\sigma_k\}_{k \neq i}$. Let us begin by fixing a site $i \in \mathcal{L}$ and another site $j \neq i$. We shall define a quantity c_{ij} that measures the strength of direct dependence of σ_i on σ_j :

$$c_{ij} \equiv \sup_{\{\sigma\}, \{\tilde{\sigma}\}: \sigma_k = \tilde{\sigma}_k \forall k \neq j} d\left(\pi_{\{i\}}(\cdot|\{\sigma\}), \pi_{\{i\}}(\cdot|\{\tilde{\sigma}\})\right), \quad (2.3)$$

where

$$d(\mu_1, \mu_2) \equiv \sup_{A \subset E} |\mu_1(A) - \mu_2(A)| = \sup_{A \subset E} [\mu_1(A) - \mu_2(A)] \quad (2.4)$$

is half the variation distance between the probability measures μ_1 and μ_2 , and the supremum in (2.3) is taken over all pairs of configurations $\{\sigma_k\}_{k \neq i}$ and $\{\tilde{\sigma}_k\}_{k \neq i}$ that differ only at the site j . The matrix $C = (c_{ij})_{i,j \in \mathcal{L}}$ is called *Dobrushin's interdependence matrix*. Please note that c_{ij} is a “worst-case” measure of the dependence of σ_i on σ_j , in the sense that it is defined via the *supremum* over all configurations of the spins $\{\sigma_k = \tilde{\sigma}_k\}_{k \neq i}$, σ_j and $\tilde{\sigma}_j$. Finally, we define the *Dobrushin constant*

$$\alpha \equiv \sup_{i \in \mathcal{L}} \sum_{j \neq i} c_{ij}. \quad (2.5)$$

We then have the following result [1]:

Theorem 2.1 (Dobrushin uniqueness theorem) *Let Π be a quasilocal specification whose Dobrushin constant α is < 1 . Then there is at most one infinite-volume Gibbs measure for Π .*

For a proof, see [3, Section 8.1] or [4, Section V.1].⁸

Remarks. 1. Under very mild conditions on the specification Π — which always hold if, for example, the state space E is finite — it can be shown that there exists *at least one* infinite-volume Gibbs measure for Π . So the upshot of Dobrushin’s uniqueness theorem is that there exists *exactly one* infinite-volume Gibbs measure for Π .

2. There is an extension of Dobrushin’s uniqueness theorem that uses the Kantorovich–Rubinstein–Vasershtein–Ornstein distance corresponding to an arbitrary metric on the state space E , in place of the variation distance (2.4): see [2] or [4, Section V.3]. This extension is particularly useful in studying continuous-spin systems. But in the Potts case it gains nothing, as the color-permutation symmetry of the Potts Hamiltonian ensures that the variation distance is in fact the “natural” distance.

The hypotheses of Theorem 2.1 imply also a strong result on the decay of correlations in the unique infinite-volume Gibbs measure. We need a few definitions: For any function $f(\{\sigma\})$ and any site i , we define the *oscillation of f at i* :

$$\delta_i(f) \equiv \sup_{\{\sigma\}, \{\sigma'\}: \sigma_k = \sigma'_k \ \forall k \neq i} |f(\{\sigma\}) - f(\{\sigma'\})|. \quad (2.6)$$

We say that f has *finite total oscillation* if

$$\Delta(f) \equiv \sum_{i \in \mathcal{L}} \delta_i(f) < \infty. \quad (2.7)$$

(In particular, any bounded function depending on only finitely many spins has finite total oscillation.) Finally, let C^n be the n^{th} matrix power of Dobrushin’s interdependence matrix C , and define

$$D_{ij} \equiv \sum_{n=0}^{\infty} (C^n)_{ij}. \quad (2.8)$$

We then have:

Theorem 2.2 *Let Π be a quasilocal specification satisfying the Dobrushin condition $\alpha < 1$. Then the unique infinite-volume Gibbs measure μ satisfies*

$$|\mu(fg) - \mu(f)\mu(g)| \leq \frac{1}{4} \sum_{i,j \in \mathcal{L}} \delta_i(f) D_{ij} \delta_j(g) \quad (2.9)$$

for all functions f, g of finite total oscillation.

In particular, if \mathcal{L} is a regular lattice and the interaction is of finite range (so that $c_{ij} = 0$ whenever $|i - j| > R$), then Dobrushin’s condition $\alpha < 1$ implies that D_{ij} decays *exponentially* as $|i - j| \rightarrow \infty$, so that Theorem 2.2 implies the *exponential decay of correlations* in the unique infinite-volume Gibbs measure. For proofs of Theorem 2.2 as well as these related results, see [3, Section 8.2] or [4, Section V.2].

⁸ *Warning:* Simon [4] denotes by ρ_{ji} what we have called c_{ij} — note the reversal of indices!

3 General Proof of Uniqueness for $q > 2r$

Let us now apply Dobrushin's uniqueness theorem to a q -state Potts antiferromagnet defined by the (formal) Hamiltonian

$$\mathcal{H} = - \sum_{i \sim j} J_{ij} \delta_{\sigma_i \sigma_j} \quad (3.1)$$

with all couplings satisfying $-\infty \leq J_{ij} \leq 0$. We say that j is a nearest neighbor of i (denoted $j \sim i$) in case $J_{ij} \neq 0$. We need to calculate the Dobrushin interdependence constants c_{ij} .

First, some preliminaries: Let ρ be a probability measure on the state space E , and let $f \geq 0$ be any function on E such that $\rho(f) \equiv \int f d\rho > 0$. Then we define the probability measure $\rho^{(f)}$ by

$$\rho^{(f)} = \frac{f\rho}{\rho(f)} \quad (3.2)$$

(" ρ weighted by f and then normalized").

Lemma 3.1 *Let $0 \leq f, g \leq 1$. Then*

$$d(\rho^{(f)}, \rho^{(g)}) \leq \max \left[\frac{\rho(1-f)}{\rho(f)}, \frac{\rho(1-g)}{\rho(g)} \right]. \quad (3.3)$$

PROOF. By definition,

$$d(\rho^{(f)}, \rho^{(g)}) = \sup_{ACE} \int_A \left[\frac{g(x)}{\rho(g)} - \frac{f(x)}{\rho(f)} \right] d\rho(x). \quad (3.4)$$

Suppose (without loss of generality) that $\rho(f) \leq \rho(g)$. Then $1/\rho(f) \geq 1/\rho(g)$, so that

$$\frac{g(x)}{\rho(g)} - \frac{f(x)}{\rho(f)} \leq \frac{1-f(x)}{\rho(f)} - \frac{1-g(x)}{\rho(g)} \quad (3.5)$$

$$\leq \frac{1-f(x)}{\rho(f)} \quad [\text{since } g \leq 1]. \quad (3.6)$$

But since $f \leq 1$, we have $\int_A [1-f(x)] d\rho(x) \leq \int_E [1-f(x)] d\rho(x) \equiv \rho(1-f)$. ■

Remark. 1. If $\rho(f) = \rho(g)$ and the supports of $1-f$ and $1-g$ are disjoint, then this estimate is sharp.

Let us now apply this lemma to compute the Dobrushin constant c_{ij} in the Potts antiferromagnet (3.1). We shall assume that the site i has at most r nearest neighbors. Fix two configurations $\{\sigma_k\}_{k \neq i}$ and $\{\tilde{\sigma}_k\}_{k \neq i}$ that differ only at the site j . Let ρ be

the conditional probability distribution at site i in the presence of all of i 's neighbors *other than* j :

$$\rho(\sigma_i) = \frac{\exp\left[\sum_{k \neq i, j} J_{ik} \delta_{\sigma_i \sigma_k}\right]}{\sum_{\sigma=1}^q \exp\left[\sum_{k \neq i, j} J_{ik} \delta_{\sigma \sigma_k}\right]} . \quad (3.7)$$

And let

$$f(\sigma_i) = \exp[J_{ij} \delta_{\sigma_i \sigma_j}] \quad (3.8a)$$

$$g(\sigma_i) = \exp[J_{ij} \delta_{\sigma_i \tilde{\sigma}_j}] \quad (3.8b)$$

The antiferromagnetic condition $J_{ij} \leq 0$ guarantees that $0 \leq f, g \leq 1$, so we can apply Lemma 3.1. Because the site i has at most $r - 1$ nearest neighbors $k \neq j$, it follows that in the measure ρ there are at least $q - r + 1$ states with equal weight (namely, those states not equal to any of the $\{\sigma_k\}_{k \neq i, j}$). Moreover, since all the J_{ik} are ≤ 0 , all the states that *are* equal to one or more of the $\{\sigma_k\}_{k \neq i, j}$ have *smaller* weight. Hence the maximum weight given by ρ to any single state is $\leq 1/(q - r + 1)$. Furthermore, $1 - f$ is nonzero on at most one state (namely, σ_j) and is there ≤ 1 ; so we have $\rho(1 - f) \leq 1/(q - r + 1)$. The same holds for $\rho(1 - g)$. Hence, by Lemma 3.1,

$$d(\rho^{(f)}, \rho^{(g)}) \leq \max\left[\frac{\rho(1 - f)}{\rho^{(f)}}, \frac{\rho(1 - g)}{\rho^{(g)}}\right] \leq \frac{1}{q - r} , \quad (3.9)$$

so that

$$c_{ij} \leq \frac{1}{q - r} \quad (3.10)$$

and consequently

$$\sum_{j \sim i} c_{ij} \leq \frac{r}{q - r} . \quad (3.11)$$

If we now assume that *every* site in the lattice has at most r nearest neighbors, we can conclude that

$$\alpha \equiv \sup_{i \in \mathcal{L}} \sum_{j \sim i} c_{ij} \leq \frac{r}{q - r} . \quad (3.12)$$

In particular, Dobrushin's condition $\alpha < 1$ holds whenever $q > 2r$. Moreover, the bound (3.12) holds *uniformly* in the values of the couplings $\{J_{ij}\}$, provided only that they are antiferromagnetic. Therefore, Theorems 2.1 and 2.2 guarantee that for $q > 2r$ there exists a unique infinite-volume Gibbs measure at all temperatures (including zero temperature), and that this unique infinite-volume Gibbs measure exhibits exponential decay of correlations uniformly in the temperature.

Remarks. 1. For the Potts antiferromagnet at *zero* temperature, i.e. when all nonzero J_{ij} equal $-\infty$, the bound (3.10) is sharp.

2. Kotecký (cited in [3, pp. 148–149, 457]) obtained the result (3.10)–(3.12) *at zero temperature*. But at nonzero temperature he obtained the weaker result $c_{ij} \leq 2/(q - r)$ and hence $\alpha \leq 2r/(q - r)$, so that he proved uniqueness only for $q > 3r$.

4 Improvements via Single-Site Decimation

In this section we are going to improve on the bound $q > 2r$, using a computer-assisted proof that must be carried separately for each lattice. For each of the four lattices we study (square, hexagonal, triangular, and Kagomé) we find that uniqueness holds for $q > 2r - 2$. But of course there is no guarantee that this result holds for general lattices!

We emphasize that our proof in this section is valid only at zero temperature ($J = -\infty$). Presumably the result holds also for finite $-\infty < J < 0$, but we do not have any proof of this fact.

The idea of our proof is simple: decimate the original lattice and then apply Dobrushin’s criterion to the decimated lattice. This trick has also been used by other authors in a different context [38].

The decimation step can be expressed in a general fashion. Consider a spin s that interacts with r nearest-neighbor spins t_1, \dots, t_r . (See Figure 4 for the case of the square lattice, which has $r = 4$.) We have to perform the sum $\sum_{s=1}^q \exp(J \sum_j \delta_{s,t_j})$; this will give us the statistical weight associated after decimation to the spin configuration (t_1, \dots, t_r) . The result is very simple for the antiferromagnetic model at zero temperature (that is, $J = -\infty$):

$$\sum_{s=1}^q \exp\left(J \sum_{j=1}^r \delta_{s,t_j}\right) \stackrel{J=-\infty}{=} \sum_{s=1}^q \prod_{j=1}^r (1 - \delta_{s,t_j}) = q - C(t_1, \dots, t_r), \quad (4.1)$$

where $C(t_1, \dots, t_r)$ is the number of distinct spin values (“colors”) we have in the configuration (t_1, \dots, t_r) . Thus, decimating the spin s will generate the r -body interaction (4.1) among the spins t_1, \dots, t_r .

In this section we will be considering only regular lattices, in which each site has the same number r of nearest neighbors.

4.1 Square lattice

In this case the original lattice is bipartite, so we can sum over all the spins belonging to one of the two sublattices (for instance, the empty circles in Figure 5). In this way we obtain a decimated lattice defined by the rest of the original spins (solid circles in Figure 5). This decimated lattice is again a square lattice, but rotated 45 degrees with respect to the original one.

The previous discussion on the decimation procedure tells us that the interaction on the decimated lattice lives on the “plaquettes” (= squares): the statistical weight for each such square is given by (4.1). Each spin t_0 on the decimated lattice (see Figure 5) interacts with the other eight spins located on the four squares to which t_0 belongs: (t_0, t_1, t'_2, t_2) , (t_0, t_2, t'_3, t_3) , (t_0, t_3, t'_4, t_4) , and (t_0, t_4, t'_1, t_1) . These eight spins fall into two classes: four nearest-neighbor spins t_1, t_2, t_3, t_4 (which belong simultaneously to two of those squares), and four next-to-nearest neighbors t'_1, t'_2, t'_3, t'_4 (which belong to only one of those squares). Thus, the quantity

$$c_{0,j} \equiv \sup_{\{t\}, \{\tilde{t}\}: t_k = \tilde{t}_k \forall k \neq j} d\left(\rho_0(\cdot | \{t\}), \rho_0(\cdot | \{\tilde{t}\})\right) \quad (4.2)$$

will depend on whether the spin t_j is a nearest neighbor or a next-to-nearest neighbor of the spin t_0 . In what follows, $c_{0,\text{nn}}$ will denote this quantity evaluated at a nearest-neighbor spin t_j , and $c_{0,\text{nnn}}$ will denote the same quantity evaluated at a next-to-nearest-neighbor spin t_j .

To obtain $c_{0,j}$ we have to consider all the q^8 distinct configurations $\{t\}$ of the spins $t_1, t_2, t_3, t_4, t'_1, t'_2, t'_3, t'_4$, compute the conditional probability measure $\rho_0(\cdot|\{t\})$ for each such configuration $\{t\}$, compute the variation distance between all pairs of such measures whose second arguments differ only by the value of the spin t_j , and finally take the maximum of those distances. In the original proof of Kotecký one could easily figure out which were the configurations which maximize (4.2). Here, this is more complicated due to the form of the 4-body interaction (4.1). The important point is that for each fixed q there is only a *finite* number of configurations to look at. So we can write a computer algorithm to examine all the possible configurations and compute (4.2). We have written a FORTRAN code implementing these ideas. In this case, the number of configurations is manageable, but in order to streamline the computation we have exploited the color-permutation symmetry of the Potts Hamiltonian and have considered only those configurations that are not related by a mere relabeling of the colors. This list of configurations was generated by another FORTRAN code using a recursive algorithm.⁹

For each q we obtained $c_{0,\text{nn}}$ and $c_{0,\text{nnn}}$. Given these values it is easy to compute the quantity

$$\alpha \equiv \sum_{j \neq 0} c_{0,j} = 4c_{0,\text{nn}} + 4c_{0,\text{nnn}}. \quad (4.3)$$

When $\alpha < 1$, Dobrushin's theorem states that the infinite-volume Gibbs measure is unique and that this measure exhibits exponentially decaying correlations. We performed this computation for $q = 5, 6, 7, 8$. [The case $q = 4$ is very special. First, the statistical weight (4.1) associated to a plaquette with all the spins in different colors (i.e. $C = 4 = q = r$) is zero. Second and more important, there are configurations of the spins $t_1, \dots, t_4, t'_1, \dots, t'_4$ for which *all* possible values of t_0 are forbidden at $T = 0$, so that the probability measure $\rho_0(\cdot|\{t\})$ at $T = 0$ is ill-defined. In this case, we would have to compute $\rho_0(\cdot|\{t\})$ at $T > 0$ and then take the limit $T \rightarrow 0$. We are not going to consider such pathological cases in this paper.¹⁰]

The numerical results for $q = 5, 6, 7, 8$ are displayed in Table 2. Moreover, the general formulae for $q \geq 6$ can be easily guessed. The method is as follows: First, we identify which are the configurations that maximize $c_{0,\text{nn}}$ for each value of q . There is (empirically) a value of $q = q_{\text{min}}^{\text{nn}}$ such that whenever $q \geq q_{\text{min}}^{\text{nn}}$ we always find the same maximizing configurations for $c_{0,\text{nn}}$. For these configurations we can compute exactly the value of $c_{0,\text{nn}}$ for general $q \geq q_{\text{min}}^{\text{nn}}$. The same procedure can be carried out for

⁹Given a list of all the possible configurations (not related by a permutation of the colors) for n spins, it is very simple to construct the same list for $n+1$ points. The starting point of the algorithm is trivial: for one spin there is only one such configuration.

¹⁰In any case, we shall see (empirically for our lattices) that Dobrushin's criterion is never satisfied when $q = r+1$. As α seems (again empirically) to be a decreasing function of q , Dobrushin's criterion would not hold when $q = r$.

$c_{0,\text{nnn}}$. For the square lattice we find that $q_{\text{min}}^{\text{nn}} = 6$ and $q_{\text{min}}^{\text{nnn}} = 5$. The configurations found to maximize $c_{0,\text{nn}}$ and $c_{0,\text{nnn}}$ are depicted in Table 3. From these patterns it is very easy to compute the general formulae:

$$c_{0,\text{nn}} = \frac{(q-3)^2(2q-7)}{q^5 - 16q^4 + 108q^3 - 391q^2 + 764q - 639} \quad \text{for } q \geq 6 \quad (4.4)$$

$$c_{0,\text{nnn}} = \frac{(q-3)^3}{q^5 - 16q^4 + 108q^3 - 389q^2 + 749q - 611} \quad \text{for } q \geq 5 \quad (4.5)$$

These results show that Dobrushin's condition $\alpha < 1$ holds for $q \geq 7$. This value is two units smaller than the value obtained by Kotecký ($q \geq 9$), although still far from the truth ($q \geq 4$, or more precisely $q > 3$).

4.2 Hexagonal lattice

This lattice is also bipartite, so we can again sum over one of the two sublattices (empty circles in Figure 6). By this decimation process we obtain a triangular lattice (solid circles in Figure 6). The statistical weight (4.1) consists of 3-body interactions living on the triangles that contain a decimated spin in their interior. To each spin t_0 there correspond three such triangles: (t_0, t_1, t_2) , (t_0, t_3, t_4) , and (t_0, t_5, t_6) ; so t_0 interacts with six nearest-neighbor spins. All these spins are equivalent, so in this case we only have to compute one quantity $c_{0,\text{nn}}$. We then have $\alpha = 6c_{0,\text{nn}}$.

The numerical results for $q = 4, 5, 6$ are contained in Table 4. The general form of $c_{0,\text{nn}}$ can be guessed from the configuration which minimizes $c_{0,\text{nn}}$ for $q \geq 4$; this configuration is shown in Table 5. The formula for $c_{0,\text{nn}}$ is

$$c_{0,\text{nn}} = \frac{(q-2)^2}{q^4 - 9q^3 + 33q^2 - 59q + 43} \quad \text{for } q \geq 4. \quad (4.6)$$

We see that Dobrushin's condition $\alpha < 1$ holds for $q \geq 5$. We again improve Kotecký's result ($q \geq 7$) by two units. This should be compared to the believed exact result $q \geq 3$ (more precisely, $q > 2.618\dots$).

4.3 Triangular lattice

This lattice is tripartite. We can decimate it by summing over all the spins belonging to one of the three sublattices (empty circles in Figure 7). The result of the decimation process is a hexagonal lattice (solid circles in Figure 7). From (4.1) we see that the interaction lives now on the hexagonal faces of this lattice, so each spin t_0 interacts with the other 12 spins belonging to the three hexagons to which t_0 belongs: $(t_0, t_1, t'_1, t'_2, t'_3, t_2)$, $(t_0, t_2, t'_4, t'_5, t'_6, t_3)$, and $(t_0, t_3, t'_7, t'_8, t'_9, t_1)$. There are two types of neighboring spins: nearest-neighbor spins t_1, t_2, t_3 (which belong to two different hexagons), and next-to-nearest neighbors t'_1, \dots, t'_9 (which belong to only

one hexagon).¹¹ For each type we have to compute the corresponding quantity (4.2). We again denote these $c_{0,\text{nn}}$ and $c_{0,\text{nnn}}$, respectively. The quantity α can be written as $\alpha = 3c_{0,\text{nn}} + 9c_{0,\text{nnn}}$.

There is one important point concerning this lattice. In the previous two examples the links of the decimated lattice did not coincide with those of the original lattice. However, in the triangular lattice the links of the decimated lattice are a *subset* of the links of the original lattice. This means that the statistical weight associated to a given hexagon is not given merely by (4.1); one has also the 2-body interactions from the original Hamiltonian. For example, the weight associated at $T = 0$ to the hexagon $(t_0, t_1, t'_1, t'_2, t'_3, t_2)$ is not $q - C(t_0, t_1, t'_1, t'_2, t'_3, t_2)$, but rather

$$[q - C(t_0, t_1, t'_1, t'_2, t'_3, t_2)](1 - \delta_{t_0, t_1})(1 - \delta_{t_1, t'_1})(1 - \delta_{t'_1, t'_2})(1 - \delta_{t'_2, t'_3})(1 - \delta_{t'_3, t_2})(1 - \delta_{t_2, t_0}). \quad (4.7)$$

When we take account of the three hexagons adjoining t_0 , we have to include 15 factors $1 - \delta_{t_k, t_j}$ in our statistical weight. However, only the three factors $(1 - \delta_{t_0, t_1})(1 - \delta_{t_0, t_2})(1 - \delta_{t_0, t_3})$ are essential. This is because those delta functions whose arguments are both distinct from t_0 are simply boundary conditions (their values are independent of t_0). If their product is non-zero, they will factor out when computing ρ_0 . If their product is zero, then we should go to $T > 0$ [where the corresponding weight $\exp(J\delta_{t_k, t_j})$ is nonzero], do the computation (and factor their contribution out), and take the limit $T \rightarrow 0$. At the end, the result would be the same as if we had omitted these factors from the very beginning.

The numerical results for $7 \leq q \leq 12$ are displayed in Table 6. We find that there are two different types of configurations maximizing $c_{0,\text{nn}}$, and only one for $c_{0,\text{nnn}}$; these patterns are depicted in Table 7. Using the configurations represented in Table 7, it is very easy to guess the general formulae for $c_{0,\text{nn}}$ and $c_{0,\text{nnn}}$:

$$c_{0,\text{nn}} = \frac{(q-5)^3}{q^4 - 21q^3 + 168q^2 - 609q + 847} \quad \text{for } q \geq 7 \quad (4.8)$$

$$c_{0,\text{nnn}} = \frac{(q-5)^3}{q^4 - 21q^3 + 168q^2 - 608q + 841} \quad \text{for } q \geq 7 \quad (4.9)$$

We see that Dobrushin's condition $\alpha < 1$ holds for $q \geq 11$, which is again an improvement of two units compared to Kotecký's result ($q \geq 13$). Our result should be compared with the expected exact value $q \geq 5$ (or more precisely $q > 4$).

4.4 Kagomé lattice

In this case we sum over those spins situated on the top vertex of the up-pointing triangles (open circles in Figure 8). After decimation we obtain a square lattice defined by the solid circles in Figure 8. Obviously the interaction (4.1) lives on the "crossed" squares (i.e. those which have a decimated spin, indicated by an open circle, inside).

¹¹ *Geometrically* there are two classes of next-to-nearest-neighbor spins: those diametrically opposite to t_0 (e.g. t'_2) and those not (e.g. t'_1 and t'_3). But these two classes play identical roles in the interaction (4.1), which is invariant under permutations of t_1, \dots, t_r .

Each spin t_0 interacts with two such squares: (t_0, t_1, t'_1, t'_2) and (t_0, t_2, t'_3, t'_4) . Among the six spins with which t_0 interacts, we can distinguish two types: two nearest-neighbor spins (t_1 and t_2), which are connected to t_0 through an original link; and four next-to-nearest-neighbor spins (t'_1, t'_2, t'_3, t'_4), which are connected to t_0 through the plaquette interaction. We associate a different value of $c_{0,j}$ to each type of spin ($c_{0,nn}$ and $c_{0,nnn}$, respectively). The quantity α is now equal to $\alpha = 2c_{0,nn} + 4c_{0,nnn}$.

As explained in the last subsection, we have to include in the statistical weight the delta functions corresponding to the surviving original links and involving the spin t_0 . In this example there are two such factors: $(1 - \delta_{t_0, t_1})(1 - \delta_{t_0, t_2})$. The numerical results for $q = 5, 6, 7, 8$ are displayed in Table 8. The configurations which minimize $c_{0,j}$ for each type of neighbor t_j are shown in Table 9. Using the configurations depicted in Table 9, it is easy to guess the general formulae for $c_{0,nn}$ and $c_{0,nnn}$:

$$c_{0,nn} = \frac{q-3}{q^2-7q+13} \quad \text{for } q \geq 5 \quad (4.10)$$

$$c_{0,nnn} = \frac{q-3}{q^3-10q^2+35q-43} \quad \text{for } q \geq 5 \quad (4.11)$$

We see that Dobrushin's condition $\alpha < 1$ holds for $q \geq 7$. Again we obtained an improvement of two units over Kotecký's result ($q \geq 9$). Our bound $q \geq 7$ should be compared to the exact result $q \geq 4$ (or more precisely, $q > 3$).

5 Further Improvements: Cluster Decimation

In this section we present slightly better results for the hexagonal and Kagomé lattices. The idea is simple: if using single-site decimation (Section 4) we obtained improved bounds, then it is natural to expect even better results if we decimate clusters of nearby spins. This is what happens in the proof presented in Ref. [38], and it happens also in our case. Obviously, as we decimate larger clusters, the effective interaction among the remaining spins becomes more and more complicated (the effective interaction contains between 128 and 2410 terms for the three cases considered below); this fact limits the practical utility of this method. Nevertheless, we have been able to improve slightly our previous results in two cases: the hexagonal and Kagomé lattices. Our method will be explained in detail in the following subsections.

5.1 Hexagonal lattice

The first step is to choose suitable clusters of spins to be summed over. In this example we selected a subset of the hexagonal faces of the original lattice (see Figure 9). The remaining spins (solid circles) define the decimated lattice, which is again a hexagonal lattice. Each hexagonal face of this decimated lattice contains one hexagonal cluster of spins that were summed over (empty circles). It is important to notice that these clusters (of empty circles) do not have any nearest-neighbor interactions with other such clusters. So, we can perform the sum over the six spins belonging to the cluster, and obtain an effective interaction among the six spins of

the decimated lattice surrounding the cluster. However, this effective interaction is not as simple as the single-site-decimation interaction (4.1). To be able to handle it, we wrote a program in MATHEMATICA to do all the required sums. The final expression can be written as a certain linear combination of products of Kronecker delta functions. This turns to be very long and complicated, so we omit its form here.¹² We remark that this interaction has the property that even when $q = 3 = r$, every state of t_0 gets nonzero weight, irrespective of the configuration of the neighboring spins; in particular, there is no ambiguity at $T = 0$, in contrast to what happens for the single-site-decimation interaction (4.1).

The effective interaction lives on the hexagonal faces of the decimated lattice. Each spin t_0 interacts with three hexagons: $(t_0, t_1, t'_1, t''_1, t'_2, t_2)$, $(t_0, t_2, t'_3, t''_2, t'_4, t_3)$, and $(t_0, t_3, t'_5, t''_3, t'_6, t_1)$. There are three types of neighbors: three nearest-neighbor spins t_1, t_2, t_3 (which belong to two different hexagons), six second-nearest-neighbor spins t'_1, \dots, t'_6 (which belong to only one hexagon and which are not diametrically opposite to t_0), and three third-neighbor spins t''_1, t''_2, t''_3 (which belong to only one hexagon and which are diametrically opposite to t_0). We have to compute a different $c_{0,j}$ for each type of neighbor: we denote these $c_{0,1n}$, $c_{0,2n}$ and $c_{0,3n}$, respectively. The quantity (2.5) is now equal to $\alpha = 3c_{0,1n} + 6c_{0,2n} + 3c_{0,3n}$.

The numerical results for $q = 3, 4$ are displayed in Table 10. We see that Dobrushin's condition $\alpha < 1$ is satisfied for $q = 4$, so we have improved by one unit the bound of Section 4. That is, we have proven that for the hexagonal lattice at zero temperature there is exponential decay of correlations for $q \geq 4$. The expected result is $q > 2.618\dots$

5.2 Kagomé lattice

In this case, our chosen clusters will be a subset of the triangular faces of the Kagomé lattice (empty circles in Figure 10); they are not connected by any nearest-neighbor interaction. The remaining spins (solid circles) define the decimated lattice, which turns out to be hexagonal. The triangular clusters are surrounded by the “deformed” hexagonal faces of the decimated lattice. In addition, there are hexagonal faces of the original lattice which belong also to the decimated lattice. The effective interaction coming from the decimation procedure lives on the “deformed” hexagonal faces only. It has again a very complicated form, and we had to use MATHEMATICA to compute it. When $q = 4 = r$, we see that the effective interaction assigns a zero weight to a few configurations. However, there are no configurations of the neighboring spins for which *all* the possible values of t_0 are forbidden, so there is no

¹²Actually, we did not use this expression in our FORTRAN programs, as it is very memory- and time-consuming. Rather, we first classified all the possible configurations into classes with the same statistical weight. For the cases considered here, the number of classes is moderate (up to 36). The important point is that we can easily tell to which class a given configuration belongs, by measuring a few quantities (such as, for instance, the number of distinct colors of the configuration). We then devise a simple formula that reproduces the correct statistical weight. The practical procedure depends on the lattice and type of decimation considered, but it is always faster and less memory-consuming than direct use of the formula computed with MATHEMATICA.

ambiguity at $T = 0$ even in this case.

From Figure 10 we see that each spin t_0 of the decimated lattice interacts with only two “deformed” hexagons. There are four types of neighboring spins: two nearest-neighbor spins t_1, t_2 (which belong to only one hexagon), one second-nearest neighbor t'_1 (which belongs to both hexagons), four third-nearest neighbors $t''_1, t''_2, t''_3, t''_4$ (which belong to one hexagon and are not connected to t'_1), and two fourth-nearest neighbors t'''_1, t'''_2 (which belong to only one hexagon and are connected to t'_1). Notice that, in addition to the effective interaction coming from the decimation procedure, we have to include the factors $(1 - \delta_{t_0, t_1})(1 - \delta_{t_0, t_2})$ arising from the original 2-body interaction, because the links $\langle t_0, t_1 \rangle$ and $\langle t_0, t_2 \rangle$ belong also to the original lattice. To each neighbor type we associate a different $c_{0,j}$: we denote these $c_{0,1n}, c_{0,2n}, c_{0,3n}$ and $c_{0,4n}$, respectively. The quantity (2.5) takes the form $\alpha = 2c_{0,1n} + c_{0,2n} + 4c_{0,3n} + 2c_{0,4n}$.

In Table 11 we show our numerical results for $q = 4, 5, 6$. We notice that the constants for the third and fourth nearest neighbors coincide in all cases. (However, we were unable to find an analytic proof of this result. In particular, there does not appear to be any symmetry that would yield this equality.) Dobrushin’s condition $\alpha < 1$ holds for $q = 6$, improving the result of Section 4 by one unit. So, there is no phase transition at zero temperature for the Kagomé lattice when $q \geq 6$, which should be compared with the expected result $q > 3$.

We have also tried to improve these results by considering decimation of hexagonal clusters (as we did in the previous subsection). After the decimation procedure we obtained a new Kagomé lattice (rotated 90 degrees). The values of α for $q = 4, 5$ were 3.83 and 1.07, respectively, which are smaller than the corresponding values reported in Table 11. However, in both cases $\alpha > 1$. Therefore, we are unable to prove exponential decay of correlations for $q < 6$.

Acknowledgments

We wish to thank Chris Henley for sending us drafts of his work [18] prior to publication.

The authors’ research was supported in part by a M.E.C. (Spain)/Fulbright fellowship (J.S.), and by U.S. National Science Foundation grants DMS-9200719 and PHY-9520978 (J.S. and A.D.S.).

References

- [1] R.L. Dobrushin, *Theor. Prob. Appl.* **13**, 197 (1968).
- [2] R.L. Dobrushin, *Theor. Prob. Appl.* **15**, 458 (1970).
- [3] H.-O. Georgii, *Gibbs Measures and Phase Transitions* (de Gruyter, Berlin–New York, 1988).
- [4] B. Simon, *The Statistical Mechanics of Lattice Gases* (Princeton University Press, Princeton, NJ, 1993).
- [5] R.B. Potts, *Proc. Camb. Philos. Soc.* **48**, 106 (1952).
- [6] F.Y. Wu, *Rev. Mod. Phys.* **54**, 235 (1982); **55**, 315 (E) (1983).
- [7] F.Y. Wu, *J. Appl. Phys.* **55**, 2421 (1984).
- [8] J. Stephenson, *J. Math. Phys.* **5**, 1009 (1964).
- [9] I. Syozi, in *Phase Transition and Critical Phenomena*, Vol. 1, edited by C. Domb and M.S. Green (Academic Press, London, 1972).
- [10] R.J. Baxter, *Exactly Solved Models in Statistical Mechanics* (Academic Press, London–New York, 1982).
- [11] R.J. Baxter, *Proc. Roy. Soc. London* **A383**, 43 (1982).
- [12] L. Onsager, *Phys. Rev.* **65**, 117 (1944).
- [13] A. Lenard, cited in E.H. Lieb, *Phys. Rev.* **162**, 162 (1967) at pp. 169–170.
- [14] R.J. Baxter, *J. Math. Phys.* **11**, 3116 (1970).
- [15] T.T. Truong and K.D. Schotte, *J. Phys.* **A19**, 1477 (1986).
- [16] P.A. Pearce and K.A. Seaton, *Ann. Phys.* **193**, 326 (1989).
- [17] D. Kim and P.A. Pearce, *J. Phys.* **A22**, 1439 (1989).
- [18] C.L. Henley, in preparation; J.K. Burton and C.L. Henley, in preparation.
- [19] S.J. Ferreira and A.D. Sokal, *Phys. Rev.* **B51**, 6727 (1995); and in preparation.
- [20] H. Saleur, *Commun. Math. Phys.* **132**, 657 (1990).
- [21] H. Saleur, *Nucl. Phys.* **B360**, 219 (1991).
- [22] R.J. Baxter, H.N.V. Temperley and S.E. Ashley, *Proc. Roy. Soc. London* **A358**, 535 (1978).
- [23] R.J. Baxter, *J. Phys.* **A19**, 2821 (1986).

- [24] R.J. Baxter, J. Phys. **A20**, 5241 (1987).
- [25] R.J. Baxter, J. Math. Phys. **11**, 784 (1970).
- [26] A. van Enter, R. Fernández and A.D. Sokal, unpublished.
- [27] J. Adler, A. Brandt, W. Janke and S. Shmulyan, J. Phys. **A28**, 5117 (1995).
- [28] P.W. Kasteleyn and C.M. Fortuin, J. Phys. Soc. Japan **26** (Suppl.), 11 (1969).
- [29] C.M. Fortuin and P.W. Kasteleyn, Physica **57**, 536 (1972).
- [30] C.M. Fortuin, Physica **58**, 393 (1972); **59**, 545 (1972).
- [31] R.J. Baxter, S.B. Kelland and F.Y. Wu, J. Phys. **A9**, 397 (1976).
- [32] M. Takano, T. Shinjo and T. Takada, J. Phys. Soc. Japan **30**, 1049 (1971).
- [33] C. Broholm, G. Aeppli, G. Espinosa and A.S. Cooper, J. Appl. Phys. **69**, 4968 (1991).
- [34] D. Huse and A.D. Rutenberg, Phys. Rev. **B45**, 7536 (1992).
- [35] J. Kondev and C.L. Henley, “Kac–Moody Symmetries of Critical Ground States”, `cond-mat/9511102`.
- [36] A.C.D. van Enter, R. Fernández and A.D. Sokal, J. Stat. Phys. **72**, 879 (1993).
- [37] C. Preston, *Random Fields* (Springer-Verlag, Berlin, 1976).
- [38] K. Haller and T. Kennedy, “Absence of Renormalization Group Pathologies near the Critical Temperature – Two Examples”, University of Arizona preprint, `mp-arc/95-505`.

| | Range of q | | | | |
|------------------------|--------------|----------------|----------|----------|------------|
| | General | Hexagonal | Square | Kagomé | Triangular |
| Kotecký | $> 2r$ | ≥ 7 | ≥ 9 | ≥ 9 | ≥ 13 |
| Single-site Decimation | | ≥ 5 | ≥ 7 | ≥ 7 | ≥ 11 |
| Cluster Decimation | | ≥ 4 | | ≥ 6 | |
| Exact | | $> 2.618\dots$ | > 3 | > 3 | > 4 |

Table 1: Range of q for which we have proven exponential decay of correlations at zero temperature for various lattices. The first row shows the result given by Kotecký [3, pp. 148–149, 457] and slightly generalized here in Section 3. The second row gives our improved result using single-site decimation (Section 4), and the next row gives our further improvement using more sophisticated decimation schemes (Section 5). The last row (“Exact”) shows what is known or believed to be the right answer.

| q | $c_{0,nn}$ | $c_{0,nnn}$ | α |
|-----|------------|-------------|--------------|
| 5 | 0.3750 | 0.2353 | 2.4412 |
| 6 | 0.1899 | 0.1093 | 1.1967 |
| 7 | 0.1137 | 0.0636 | $0.7093 < 1$ |
| 8 | 0.0756 | 0.0415 | $0.4683 < 1$ |

Table 2: Numerical results for the square lattice. For each value of q we show the quantities $c_{0,nn}$ and $c_{0,nnn}$. Finally, we give the value of the parameter $\alpha = 4c_{0,nn} + 4c_{0,nnn}$. When $\alpha < 1$ there is a unique Gibbs measure at $T = 0$.

| $c_{0,nn}$ | | $c_{0,nnn}$ |
|------------|------------|-------------|
| | | |
| $q = 5$ | $q \geq 6$ | $q \geq 5$ |

Table 3: Configurations which maximize $c_{0,nn}$ and $c_{0,nnn}$ for the square lattice when $q \geq 5$. Each distinct letter represents a distinct spin value. The spin t_0 is denoted by an empty circle (\circ). The spin t_j is the one that has two different spin values associated to it.

| q | $c_{0,\text{nn}}$ | α |
|-----|-------------------|------------|
| 4 | 0.2667 | 1.6000 |
| 5 | 0.1233 | 0.7397 < 1 |
| 6 | 0.0699 | 0.4192 < 1 |

Table 4: Numerical results for the hexagonal lattice. For each value of q we compute the quantities $c_{0,\text{nn}}$ and $\alpha = 6c_{0,\text{nn}}$.

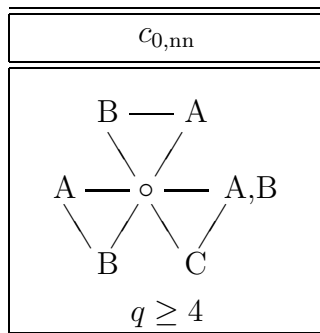


Table 5: Configurations which maximize $c_{0,\text{nn}}$ for the hexagonal lattice when $q \geq 4$. The notation is as in Table 3. Notice that, because the two outer spins within each triangle are equivalent, we can freely permute their values.

| q | $c_{0,\text{nn}}$ | $c_{0,\text{nnn}}$ | α |
|-----|-------------------|--------------------|------------|
| 7 | 0.5714 | 0.2667 | 4.1143 |
| 8 | 0.3803 | 0.1233 | 2.2504 |
| 9 | 0.2832 | 0.0699 | 1.4784 |
| 10 | 0.2244 | 0.0446 | 1.0743 |
| 11 | 0.1852 | 0.0307 | 0.8324 < 1 |
| 12 | 0.1574 | 0.0224 | 0.6741 < 1 |

Table 6: Numerical results for the triangular lattice. Notation is as in Table 2; here $\alpha = 3c_{0,\text{nn}} + 9c_{0,\text{nnn}}$.

| $c_{0,nn}$ | $c_{0,nnn}$ |
|--|--|
| <p style="text-align: center;">$q \geq 7$</p> | <p style="text-align: center;">$q \geq 7$</p> |

Table 7: Configurations maximizing $c_{0,nn}$ and $c_{0,nnn}$ for the triangular lattice when $q \geq 7$. Notation is as in Table 3. Notice that, as in Table 5, we obtain equivalent configurations by permuting the outer spins within each hexagon (i.e. those spins that are not shared between two hexagons).

| q | $c_{0,nn}$ | $c_{0,nnn}$ | α |
|-----|------------|-------------|--------------|
| 5 | 0.6667 | 0.2857 | 2.4762 |
| 6 | 0.4286 | 0.1304 | 1.3789 |
| 7 | 0.3077 | 0.0727 | $0.9063 < 1$ |
| 8 | 0.2381 | 0.0459 | $0.6597 < 1$ |

Table 8: Numerical results for the Kagomé lattice. Notation is as in Table 2; here $\alpha = 2c_{0,nn} + 4c_{0,nnn}$.

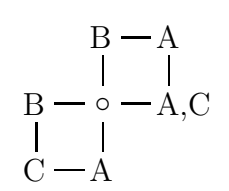
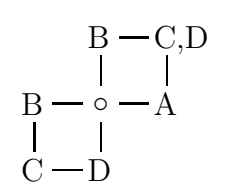
| $c_{0,nn}$ | $c_{0,nnn}$ |
|--|---|
|  <p style="margin-top: 10px;">$q \geq 5$</p> |  <p style="margin-top: 10px;">$q \geq 5$</p> |

Table 9: Configurations which maximize $c_{0,nn}$ and $c_{0,nnn}$ for the Kagomé lattice when $q \geq 5$. Notation is as in Table 3. In the pictures, a thick line represents a link belonging to the original lattice (and carrying an additional Kronecker delta term). On each square, the two spins not connected to such a link can be freely interchanged.

| q | $c_{0,1n}$ | $c_{0,2n}$ | $c_{0,3n}$ | α |
|-----|------------|------------|------------|--------------|
| 3 | 0.5685 | 0.3904 | 0.2136 | 4.5985 |
| 4 | 0.1036 | 0.0292 | 0.0164 | $0.5356 < 1$ |

Table 10: Numerical results for the hexagonal lattice when we use 6-spin decimation. For each type of neighbor we show the corresponding value $c_{0,j}$. We also show $\alpha = 3c_{0,1n} + 6c_{0,2n} + 3c_{0,3n}$. When $\alpha < 1$ there is a unique Gibbs measure at $T = 0$.

| q | $c_{0,1n}$ | $c_{0,2n}$ | $c_{0,3n}$ | $c_{0,4n}$ | α |
|-----|------------|------------|------------|------------|--------------|
| 4 | 1.0000 | 1.0000 | 0.6667 | 0.6667 | 7.0000 |
| 5 | 0.4949 | 0.1590 | 0.1003 | 0.1003 | 1.7504 |
| 6 | 0.2975 | 0.0581 | 0.0330 | 0.0330 | $0.8529 < 1$ |

Table 11: Numerical results for the Kagomé lattice when we use 3-spin decimation. Notation is as in Table 10; here $\alpha = 2c_{0,1n} + c_{0,2n} + 4c_{0,3n} + 2c_{0,4n}$.

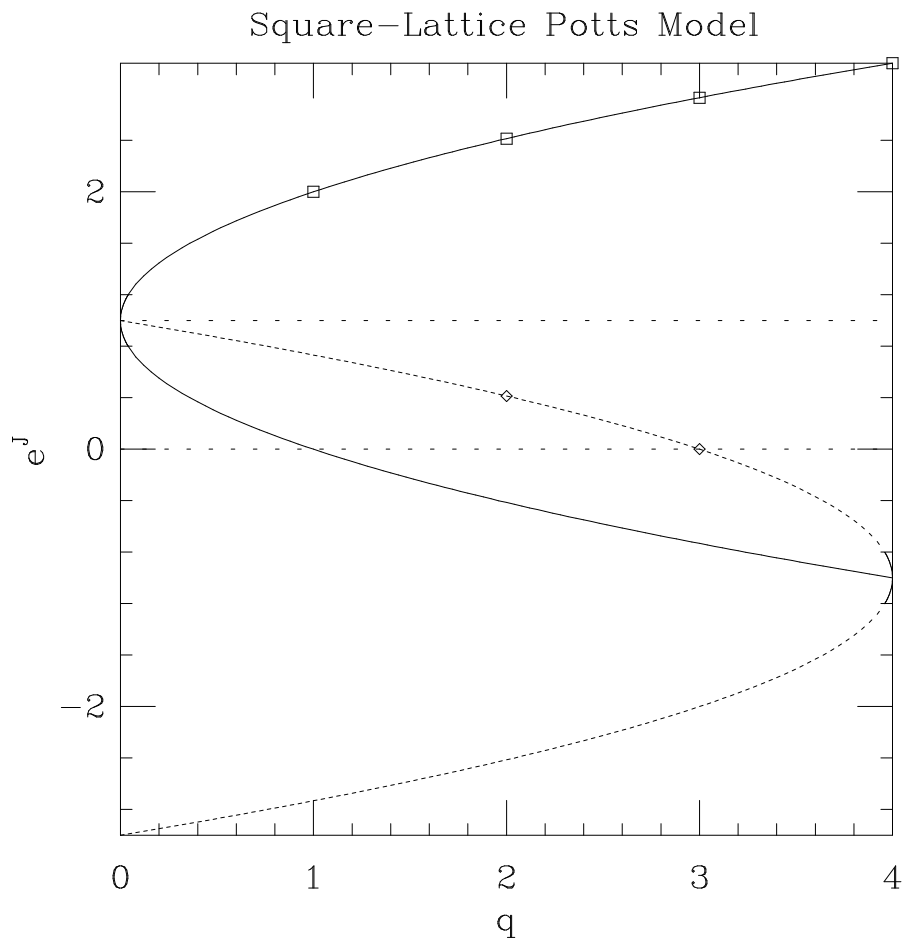


Figure 1: Curves where the square-lattice Potts model has been solved: the self-dual curve $(e^J - 1)^2 = q$ (solid curve), and $(e^J + 1)^2 = 4 - q$ (dashed curve). The horizontal dotted lines correspond to $e^J = 1$ (separating the ferromagnetic and antiferromagnetic regimes) and to $e^J = 0$ (separating the antiferromagnetic regime from the unphysical region $e^J < 0$). The squares (\square) show the known ferromagnetic critical points ($q = 1, 2, 3, 4$); and the diamonds (\diamond) mark the known antiferromagnetic critical points ($q = 2, 3$).

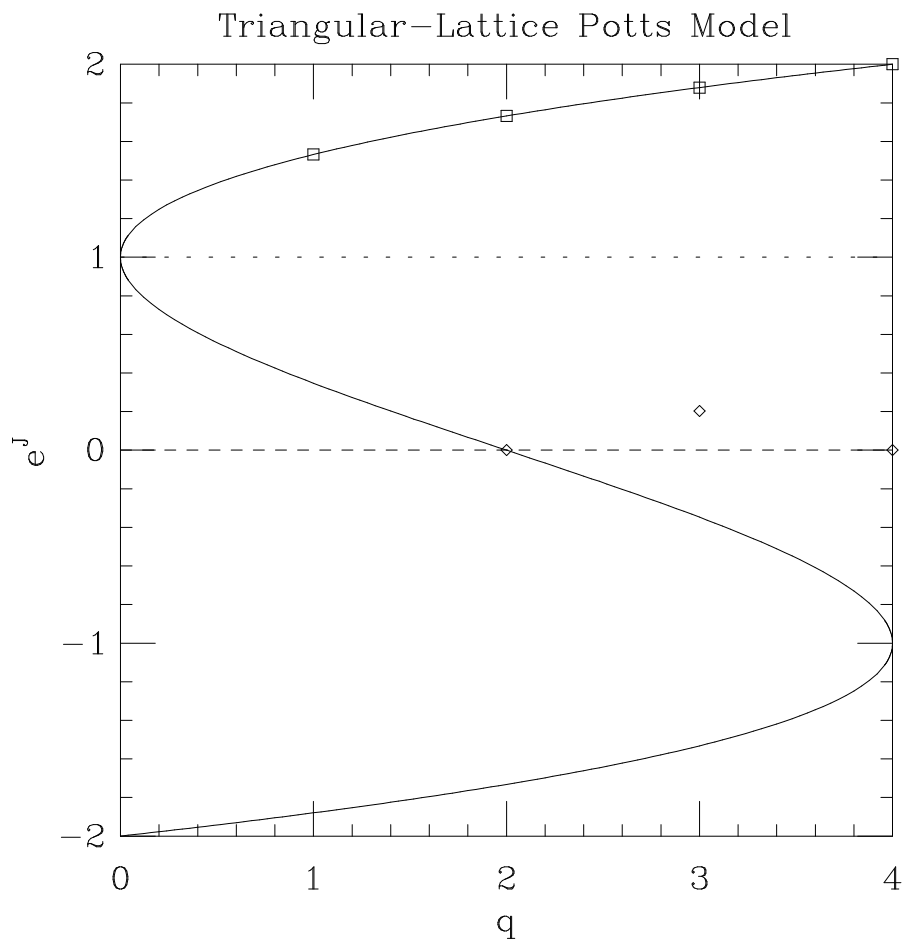


Figure 2: Curves where the triangular-lattice Potts model has been solved: $(e^J - 1)^2(e^J + 2) = q$ (solid curve), which has three branches; and the line $e^J = 0$ (dashed line). The horizontal dotted line corresponds to $e^J = 1$ (separating the ferromagnetic and antiferromagnetic regimes). The squares (\square) show the known ferromagnetic critical points ($q = 1, 2, 3, 4$); and the diamonds (\diamond) mark the known antiferromagnetic phase-transition points ($q = 2, 3, 4$). Note that the antiferromagnetic first-order transition for $q = 3$ does *not* lie on either of the exactly-solved curves.

Hexagonal-Lattice Potts Model

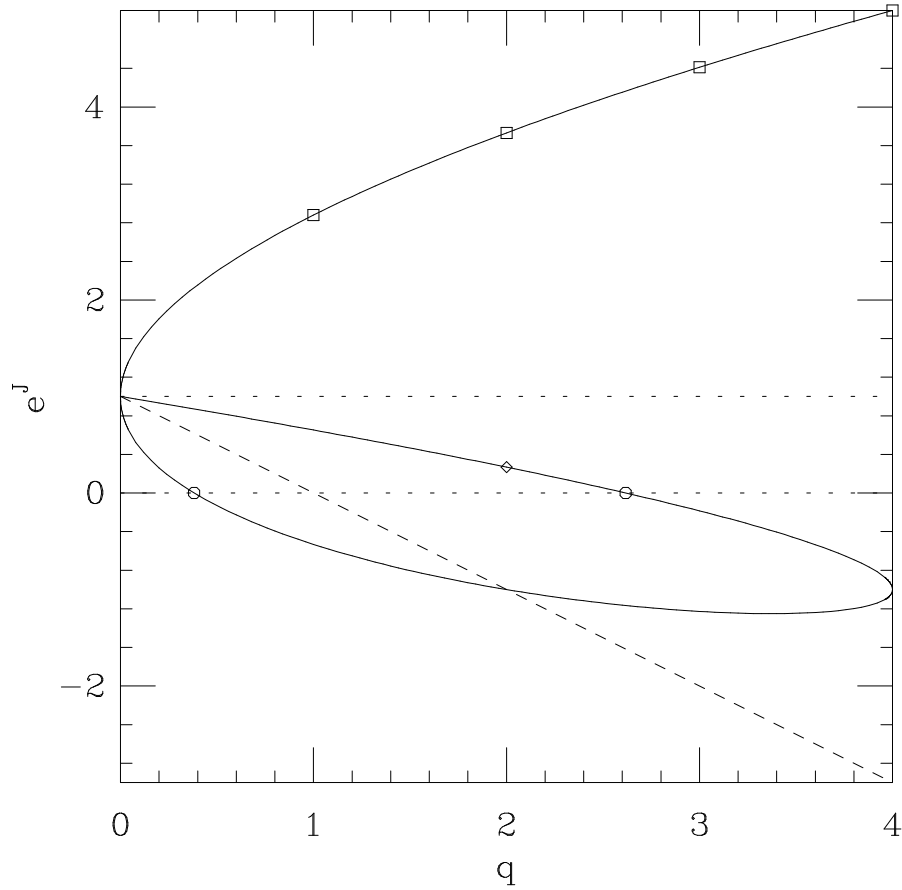


Figure 3: Curves where the hexagonal-lattice Potts model has been solved: $(e^J - 1)^3 - 3q(e^J - 1) = q^2$ (solid curve), which has three branches; and the line $e^J = 1 - q$ (dashed line). The horizontal dotted lines correspond to $e^J = 1$ (separating the ferromagnetic and antiferromagnetic regimes) and to $e^J = 0$ (separating the antiferromagnetic regime from the unphysical region $e^J < 0$). The squares (\square) show the known ferromagnetic critical points ($q = 1, 2, 3, 4$); and the diamond (\diamond) marks the known antiferromagnetic critical point for $q = 2$. The open circles (\circ) show the points where the two antiferromagnetic branches cross the $e^J = 0$ line, namely $q = (3 \pm \sqrt{5})/2$.

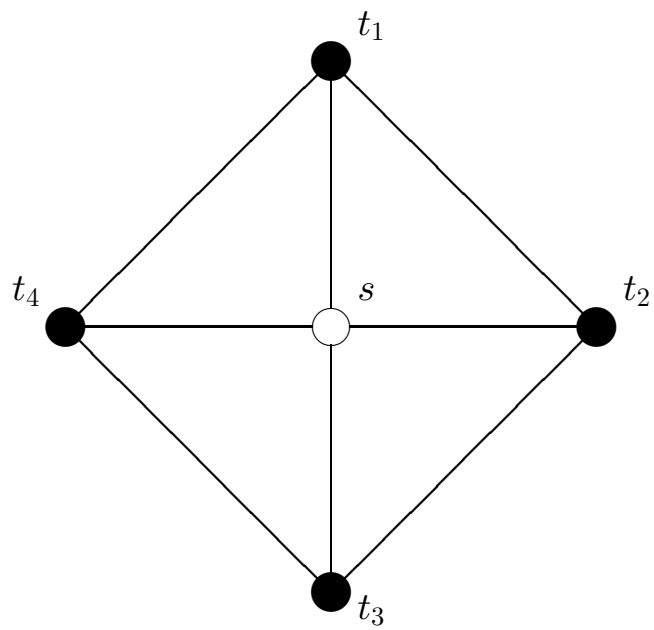


Figure 4: Decimation for the square-lattice case. Once we sum over the spin s , we obtain a new effective interaction among the spins t_j ($j = 1, 2, 3, 4$).

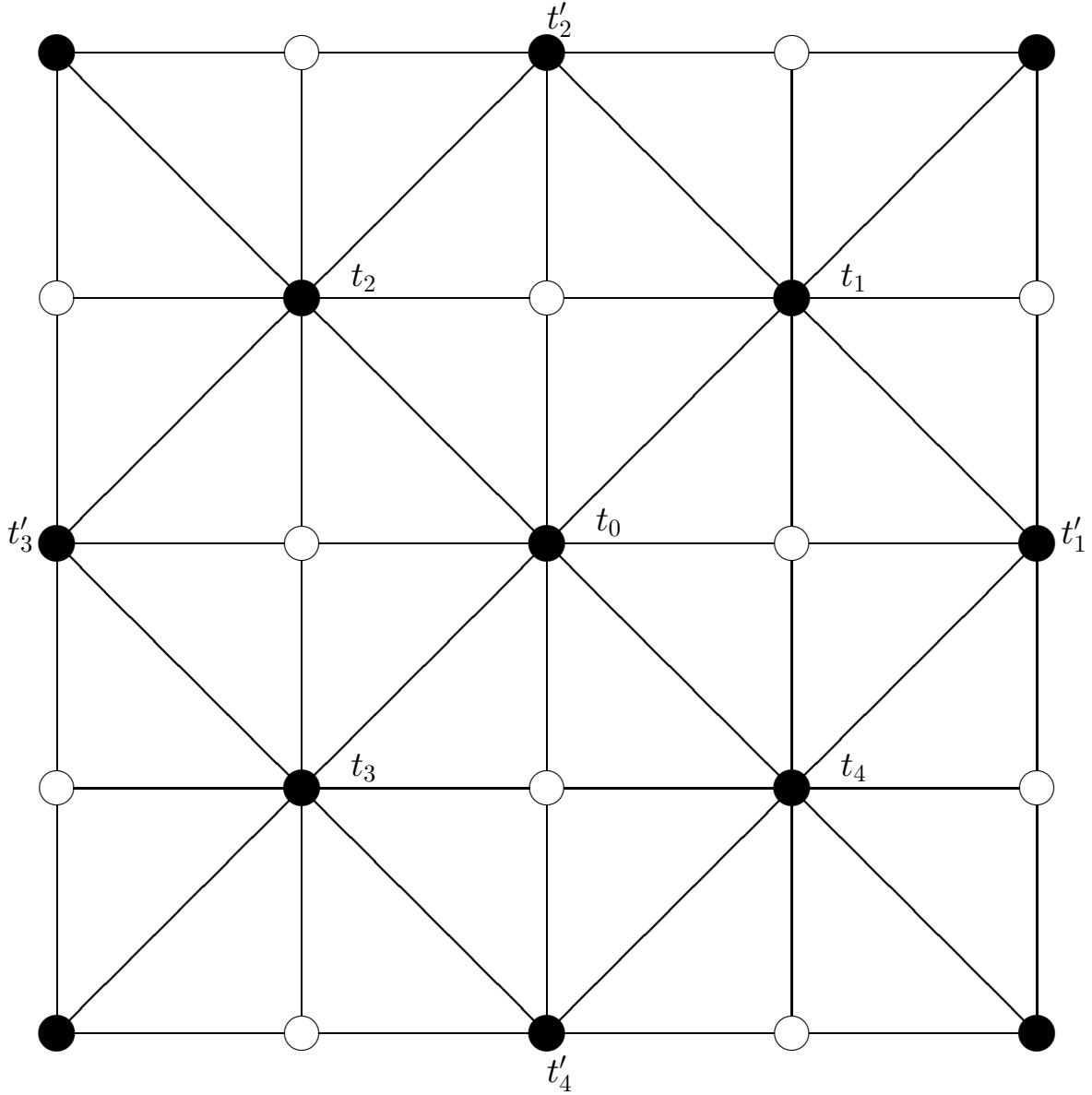


Figure 5: Decimation for the square lattice. The empty circles represent the spins summed over; the solid circles represent the resulting decimated lattice. Each spin t_0 of the decimated lattice interacts with eight spins: four nearest neighbors t_1, t_2, t_3, t_4 and four next-to-nearest neighbors t'_1, t'_2, t'_3, t'_4 .

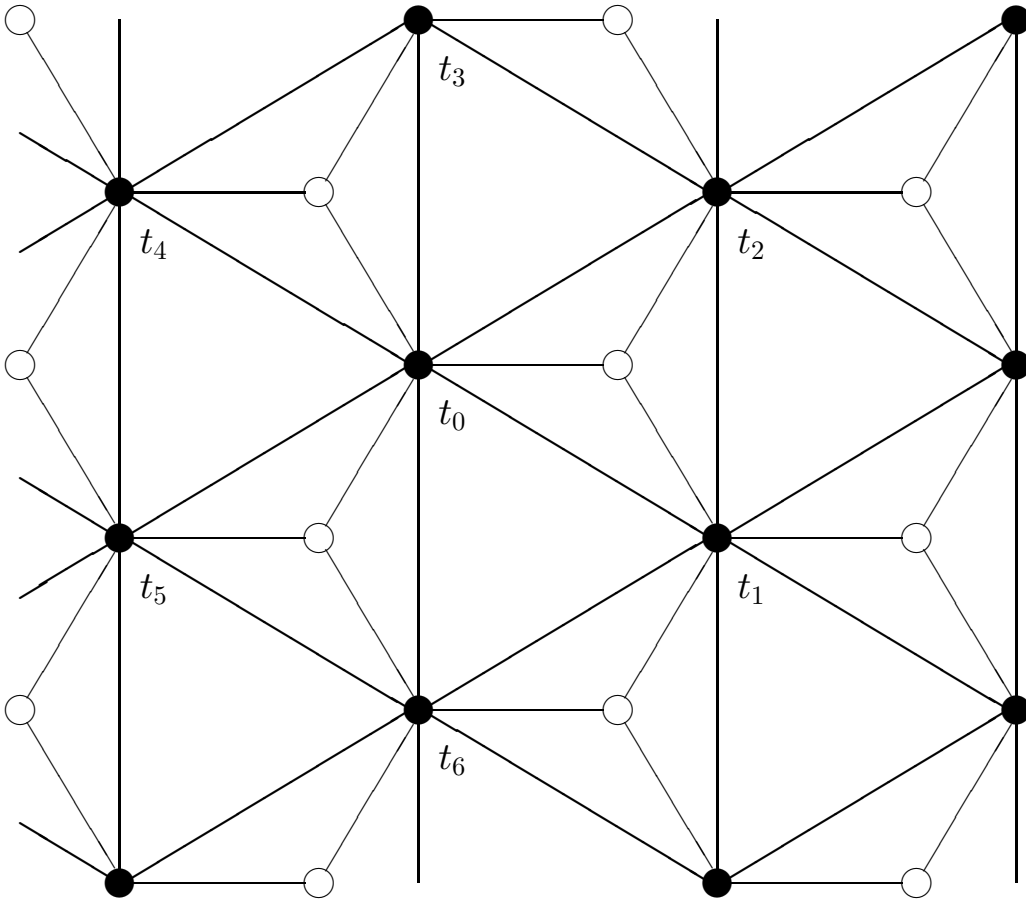


Figure 6: Decimation for the hexagonal lattice. The original hexagonal lattice is drawn with thin lines; the empty circles represent the spins summed over; the triangular lattice resulting from decimation is drawn with solid circles and thick lines. Each spin t_0 of the decimated lattice interacts with six nearest-neighbor spins t_1, \dots, t_6 .

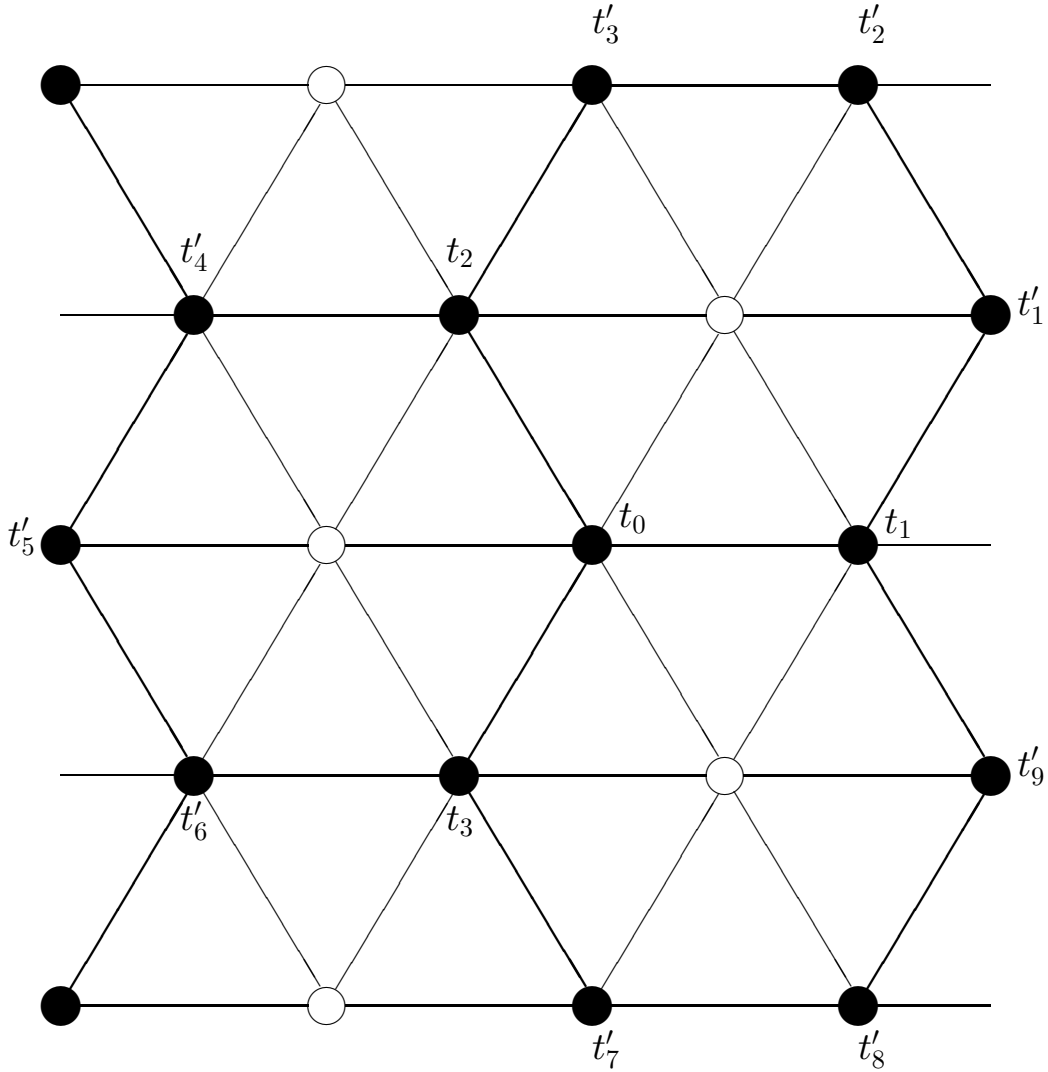


Figure 7: Decimation for the triangular lattice. The original triangular lattice corresponds to both thin and thick lines; the empty circles represent the spins summed over; the hexagonal lattice resulting from decimation is drawn with solid circles and thick lines. Each spin t_0 of the decimated lattice interacts with 12 spins: three nearest neighbors t_1, t_2, t_3 and the nine next-to-nearest neighbors t'_1, \dots, t'_9 .

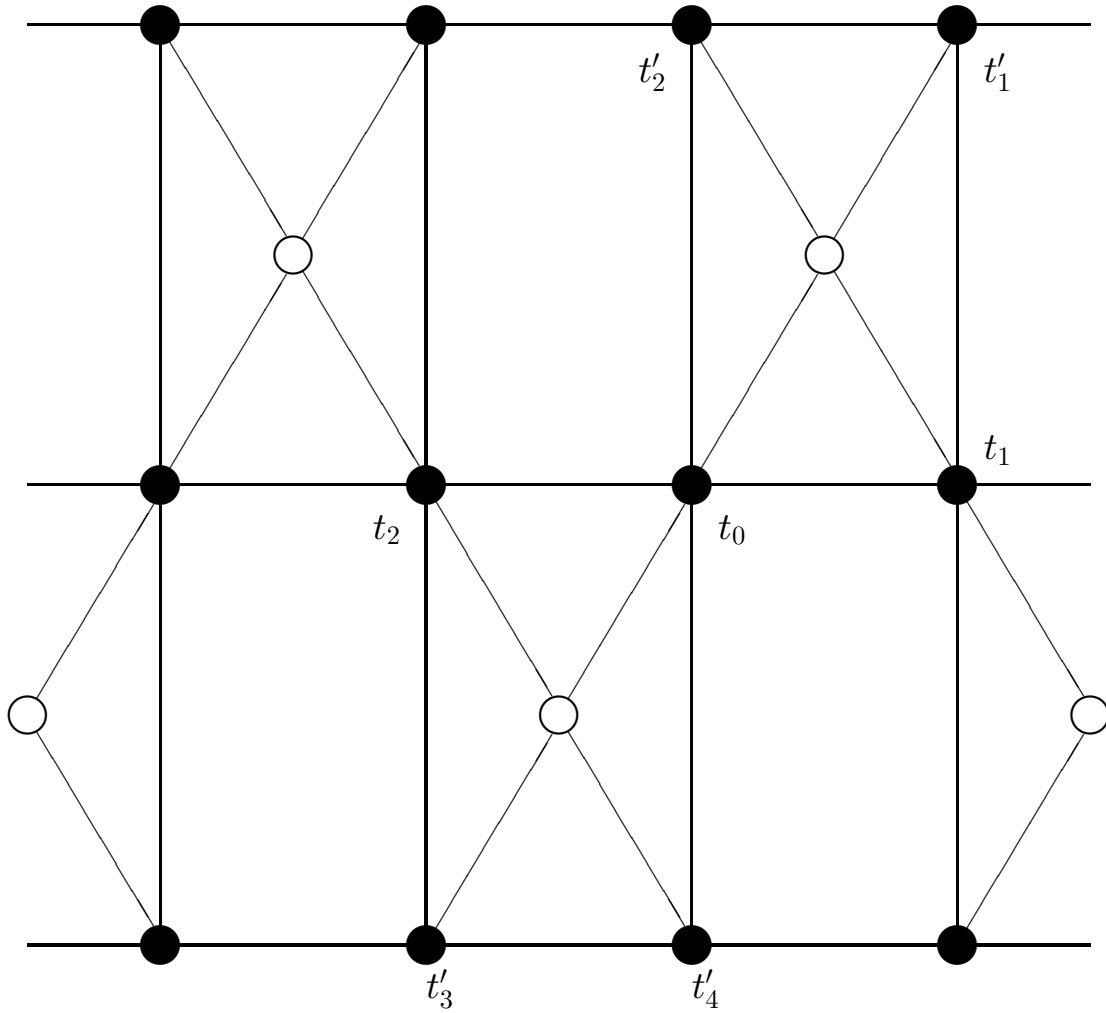


Figure 8: Decimation for the Kagomé lattice. The original Kagomé lattice corresponds to all the thin lines and the horizontal thick lines; the empty circles represent the spins summed over; the square lattice resulting from decimation is defined by the thick lines. Each spin t_0 of the decimated lattice (solid circles) interacts with 6 spins: two nearest neighbors t_1, t_2 and four next-to-nearest neighbors t'_1, t'_2, t'_3, t'_4 . All these six spins live on the two “crossed” squares to which t_0 belongs.

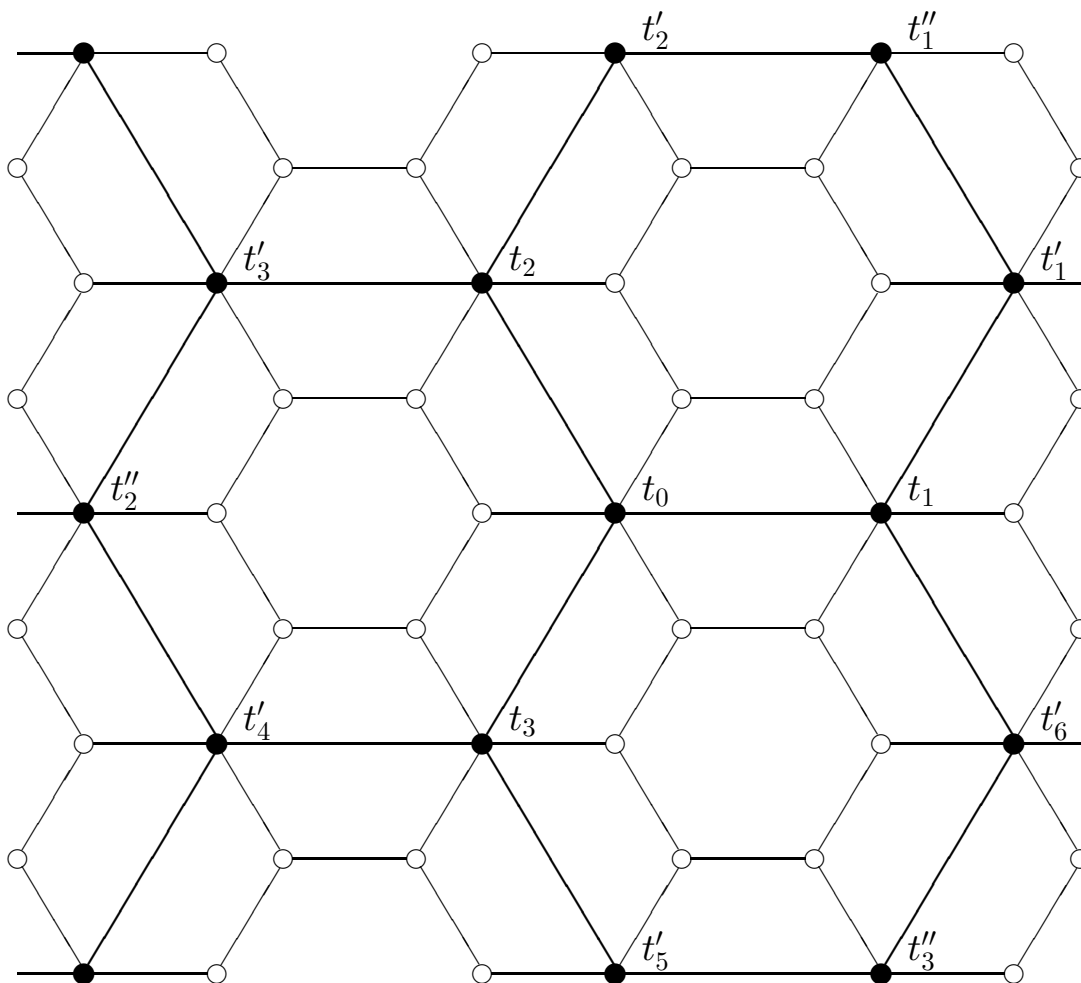


Figure 9: More complex decimation for the hexagonal lattice. The original lattice is drawn with thin lines; the empty circles represent the spins summed over; the decimated lattice is drawn with solid circles and thick lines. Each spin t_0 of the decimated lattice interacts with 12 spins: three nearest neighbors t_1, t_2, t_3 , six second-nearest neighbors t'_1, \dots, t'_6 , and three third-nearest neighbors t''_1, t''_2, t''_3 .

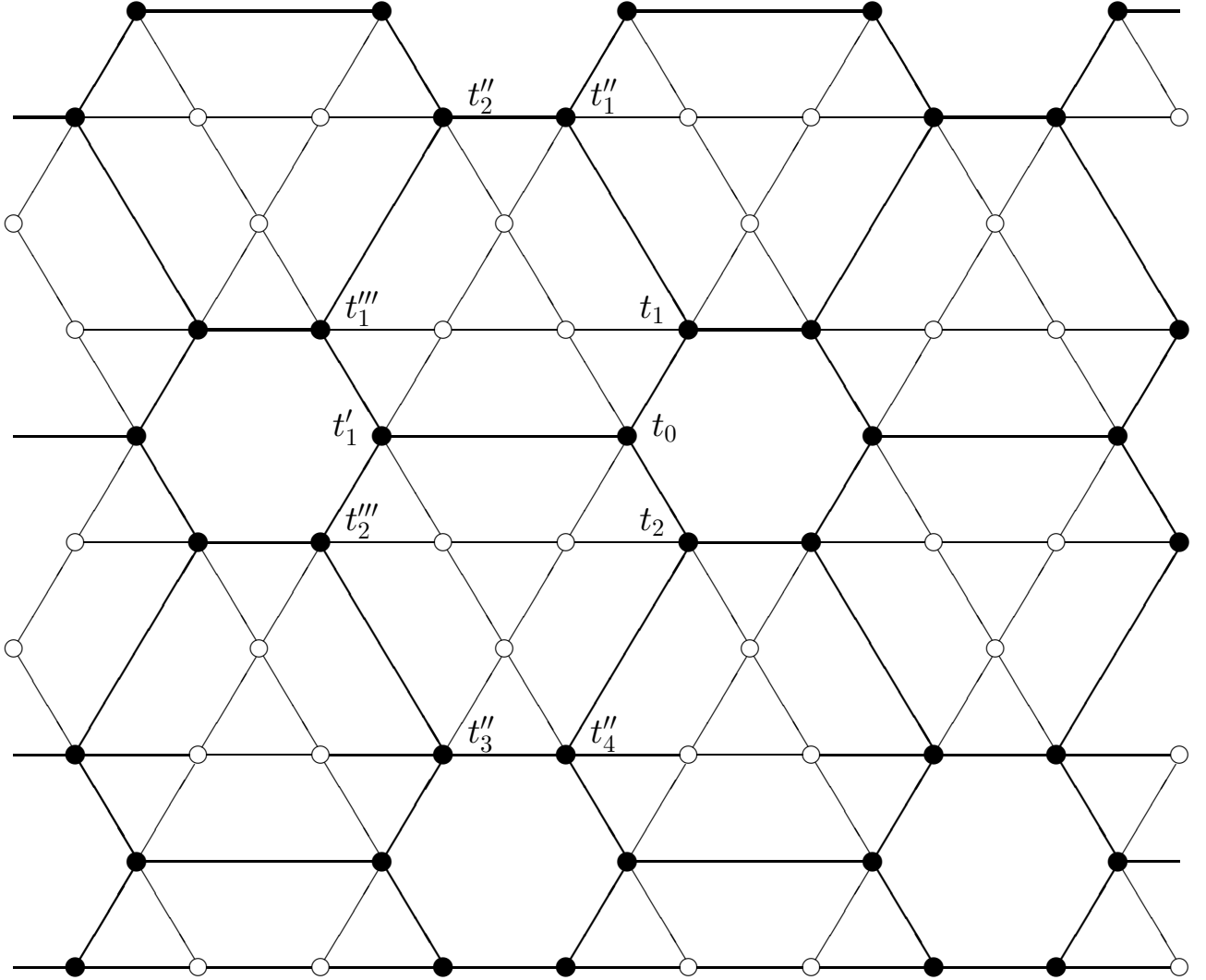


Figure 10: More complex decimation for the Kagomé lattice. The original lattice corresponds to the whole set of circles (empty and solid) and the *nearest-neighbor* bonds between them; the empty circles represent the spins summed over; the decimated lattice is drawn with solid circles and thick lines. Each spin t_0 of the decimated lattice interacts with nine spins: two nearest neighbors t_1, t_2 , one second-nearest neighbor t'_1 , four third-nearest neighbors $t''_1, t''_2, t''_3, t''_4$, and two fourth-nearest neighbors t'''_1, t'''_2 .